SCIENTIFIC REPORTS

OPEN

Hydrogen storage of $Li_4\&B_{36}$ cluster

Jiguang Du[1], Xiyuan Sun[2], Li Zhang[3], Chuanyu Zhang[4] & Gang Jiang[3]

Received: 18 October 2017
Accepted: 18 January 2018
Published online: 31 January 2018

The Saturn-like charge-transfer complex $Li_4\&B_{36}$, which was recently predicted with extensive first-principles theory calculations, were studied as a candidate for hydrogen storage material in the present work. The bonding characters of Li-B, B-B and Li-H_2 bonds were revealed by the quantum theory of atoms in molecules (QTAIM). Each Li atom in $Li_4\&B_{36}$ cluster can bind six H_2 molecules at most, which results into the gravimetric density of 10.4%. The adsorption energies of H_2 molecules on $Li_4\&B_{36}$ cluster are predicted in the range of 0.08-0.14 eV at the *w*B97*x* level of theory.

The hydrogen storage is an important issue not being solved up to now. Hydrogen can be adsorbed on a material through three different manners[1,2]. For chemisorption, the materials bind the dissociated hydrogen atoms with high binding energy of 2-4 eV, like metal hydrides and light complex hydrides[3,4]. The desorption occurs at high temperatures for the case of chemisorption. On the other hand, the materials, like nanostructured carbon[5,6], attached hydrogen molecules weakly with a binding energy in the meV range, which was regarded as physisorption. The strength of third form of binding is in the 0.1–0.8 eV range, and is intermediate between physisorption and chemisorption. Metal-decorated carbon-based nanomaterials and even their derivates[7–13], in which the metal atoms bind hydrogen in molecular form with intermediate binding energy, belong to the third form of binding. For example, the $Li_{12}C_{60}$ cluster was theoretically predicted to bind $60H_2$ at most, resulting in high gravimetric density[14], and Yoon *et al.*[15] have indicated that Ca can functionalize carbon fullerenes into high hydrogen storage capacity with a gravimetric density >8.4 wt%. In experiments, a lithium-doped fullerene with a Li:C_{60} mole ratio of 6:1 can reversibly desorb up to 5 wt % H_2 with an onset temperature of ~270 °C[16]. Deuteration of $Li_{12}C_{60}$ was determined in experiment[17], and the results indicated that up to 9.5 wt % deuterium (D_2) are absorbed in $Li_{12}C_{60}$.

Highly stable clusters were generally designed in theory for the hydrogen storage[18–20]. For example, Ba Tai *et al.*[19] have found that the B_6Li_8 cluster is a promising candidate for hydrogen storage media, which corresponds to a hydrogen uptake of 24% and adsorption energy of 0.099 eV estimated at the DFT level. Our previous work[21] indicated that the CTi_7^{2+}cluster can bind 20 H_2 molecules at most with adsorption energy of 0.24 eV, which can result into the gravimetric density of 19%. However, an ideal system is yet to be synthesized in experiment.

Boron fullerenes are also seen as efficient hydrogen storage media due to the light weight and capability to bind with metal adatoms. Many works reported the hydrogen storage of doped cage-like B_{80} with alkli-metal[22], alkaline-earth metal[23,24] and transitional metal[25]. In fact, B_{80} favors a core-shell (stuffed fullerene) structure in energy, not a cage-like configuration[26,27]. Therefore, the applications of B_{80} as hydrogen storage materials may be unrealistic. Recently, a combined experimental and theoretical study[28] observed the first borospherenes (B_{40}) with a cube-like cage structure, which brings the development of borospherene chemistry. Bai *et al.*[29] have investigated the hydrogen storage of the lithium-decorated borospherene B_{40}, and found the potential utilization of Li-B_{40} complexes as a novel nanomaterial for hydrogen storage. The Ti-decorated borospherene[30] also theoretically studied as a promising hydrogen storage material, and the evaluated reversible storage capacity is 6.1 wt% for Ti-B_{40} complexes.

A high-symmetry C_{6v} quasi-planar structure with dual π aromaticity was predicted as the ground state of B_{36}[31]. Nevertheless, by introducing four Li^+ counterions into the B_{36}^{4-} system, the neutral Saturn-like charge-transfer $Li_4\&B_{36}$ complex with D_{2h} symmetry can be highly stabilized[32]. In the present work, we will pay attention to the hydrogen storage capability of $Li_4\&B_{36}$ system.

Results and Discussion

Structures and bonding characters of $Li_4\&B_{36}$ cluster. In previous work, the extensive structural search has found that the most stable structure of $Li_4\&B_{36}$ cluster is one high-symmetry Saturn-like geometry[32]. As shown in Fig. 1, our calculations also obtained a cage structure with point group (PG) symmetry of D_{2h}, this structure corresponds to a closed-shell electronic state (ES) (^1A_g). As Table 1 shows, the average Li-B and B-B bond lengths are 2.306 Å and 1.687 Å, respectively, predicted with *w*B97*x* functional[33] in conjunction with 6-31 g

[1]College of Physical Science and Technology, Sichuan University, Chengdu, 610064, China. [2]College of Science, Sichuan Agricultural University, Ya'an, 625014, China. [3]Institute of Atomic and Molecular Physics, Sichuan University, Chengdu, 610065, China. [4]Department of Physics, Chengdu University of Technology, Chengdu, 610059, China. Correspondence and requests for materials should be addressed to J.D. (email: dujg@scu.edu.cn)

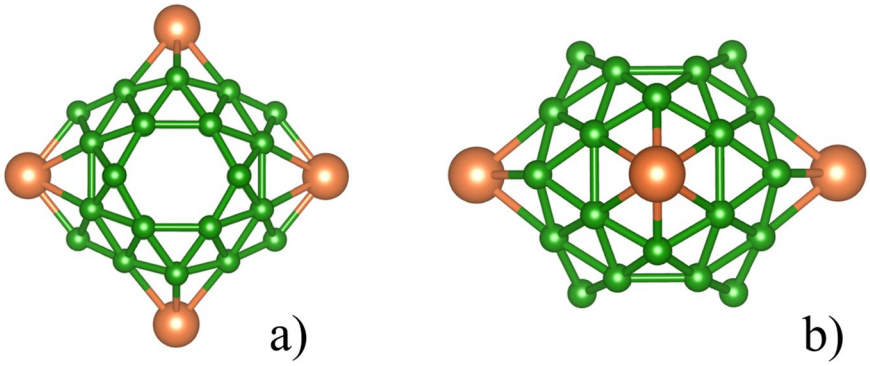

Figure 1. Relaxed structure of $Li_4\&B_{36}$ cluster (D_{2h}), a) side view, b) top view.

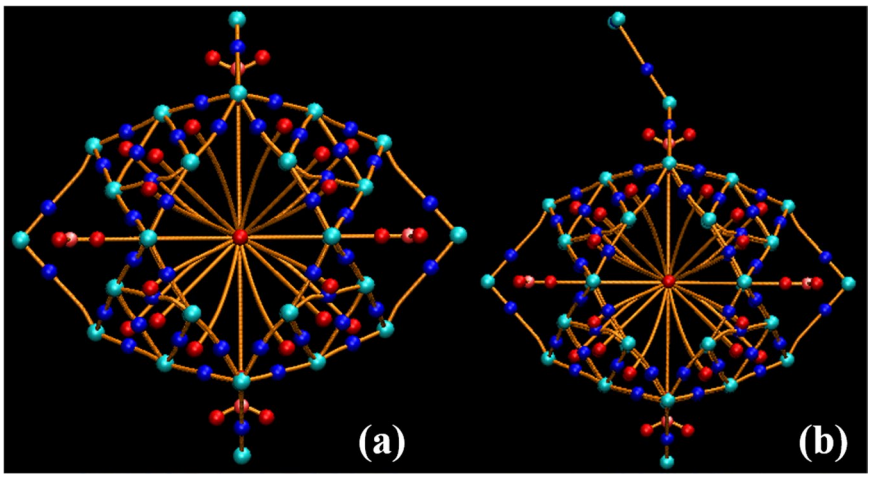

Figure 2. Molecular graph of $Li_4\&B_{36}$ (**a**) and $Li_4\&B_{36}$-H_2 (**b**) complexes. The colour scheme identifying critical points is as follows: cyan ball for attractors, blue ball for bond critical points (BCP), red ball for ring critical points (RCP).

Species		$R_{Li\text{-}B}$(Å)	$R_{B\text{-}B}$(Å)	ω_L (cm^{-1})	NICS (0)	Q_{Li} (e)	C_{Li}	E_{int} (eV)
$Li_4\&B_{36}$	This work[a]	2.306	1.687	203	−44.6	0.86	$1s^2 2s^0 2p^{0.1}$	4.09
	Theory[b]	2.266	1.690	—	−42.8	0.83		3.27

Table 1. The calculated structural parameters, the lowest frequency, NICS, NPA charge (Q_{Li}) and electron configuration (C_{Li}) of Li atoms and interaction energy (E_{int}) of bare $Li_4\&B_{36}$ cluster. [a]Our calculated values at the wB97x/6-31 G(d, p) level of theory. [a]Predicted values at the PBE0/6-311 + G(d) level of theory from ref[32].

(d, p) basis set, and the calculated bond lengths are excellent in agreement with previous results[32]. Natural population analysis (NPA)[34] charge (shown in Table 1) indicate that each face-capping Li atom donating about one electron to the electron-deficient B_{36} core acts as electron donor, resulting into the $(Li^+)_4B_{36}^{4-}$ charge-transfer complex. From the electron configuration of Li atoms (C_{Li}) in $Li_4\&B_{36}$ cluster, one can find that the charge transfer from Li to B atoms result into the empty occupancy of 2 s valence shell. The sphere aromaticity of $Li_4\&B_{36}$ is revealed by the huge negative nucleus-independent chemical shifts (NICS)[35] of -44.6 ppm at the cage centers. The lowest vibrational frequency is 203 cm^{-1} at the *w*B97*x* level of theory, which is sufficiently large to meet a stability criterion suggested by Hoffmann *et al.*[36]. The high binding energy of 4.09 eV per Li atom also confirms the high stability of $Li_4\&B_{36}$ cluster.

The bonding nature of $Li_4\&B_{36}$ cluster will be revealed with QTAIM method[37], the molecular graphs and corresponding topological parameters are given in Fig. 2 and Table 2, respectively. Different (3, -1) bond critical points (BCPs) relative to B-B bonds and the bond critical points (BCPs) between Li atoms and two neighboring B atoms are found. For the traditional topological criterion, the covalent interaction corresponds to a negative Laplacian of electron density ($\nabla^2\rho(r) < 0$) at the BCP. Another property, the total energy density $H(r)$ (defined as the sum of local kinetic energy density $G(r)$ and local potential energy density $V(r)$) proposed by Cremer and Krala[38] was proven to be very appropriate to characterize the degree of covalency of a bond. The negative $H(r)$

Species	BCP	ρ	$\nabla^2\rho$	H(r)	FBO	ELF
H_2	H-H	0.270	−1.219	−0.305	1.00	1.00
$Li_4\&B_{36}$	B-Li	0.026	0.113	0.001	0.23	0.05
	B-B	0.127 (0.151)[a]	−0.090 (−0.271)	−0.073 (−0.115)	0.56 (0.87)	0.69 (0.87)
$Li_4\&B_{36}$-H_2	B-Li	0.026	0.113	0.001	0.23	0.05
	B-B	0.127 (0.151)	−0.090 (−0.271)	−0.073 (−0.115)	0.56 (0.87)	0.69 (0.87)
	Li-H_2	0.008	0.043	0.002	0.21	0.01
	H-H	0.267	−1.190	−0.299	0.76	1.00

Table 2. Topological parameters of isolated H_2 molecule and $Li_4\&B_{36}$ cluster and H_2-adsorbed $Li_4\&B_{36}$-H_2 complex. [a]parameters for the shortest B-B bonds were shown in the parentheses.

is the indicator of a covalent bond. As Table 2 shows, all bond critical points relative to Li-B bonds correspond to positive Laplacian of electron density $\nabla^2\rho$(r) and H(r) value. This indicates that the Li-B bonds show typical closed-shell character corresponding to ionic bonds. On the other hand, the covalent bond nature of B-B bonds is revealed by their large electron density ρ(r), negative $\nabla^2\rho$(r) and H(r) values. This result is in excellent agreement with fuzzy bond order (FBO)[39] analyses, which predicts the bond order between Li and B atoms to be 0.23, suggesting the weak ionic bond nature of Li-B bonds. And the high fuzzy bond order (FBO) of B-B bonds reveal the strong covalent interaction between the bonding B atoms. The topological parameters of electron density shown in Table 2 indicate that all Li-B and B-B chemical bonds in $Li_4\&B_{36}$ show typical ionic and covalent natures, respectively, which is also supported by the electron localization function (ELF)[40,41] shown in Table 2.

H_2 adsorption on $Li_4\&B_{36}$ cluster. In this section, we will pay attention to the hydrogen storage stability of $Li_4\&B_{36}$ cluster. The bond length of free H_2 molecule is predicted as 0.744 Å at the *w*B97*x*/6-31 g (d, p) level of theory, and is in agreement with the experimental value of 0.741 Å[42]. The free and adsorbed H_2 molecules in $Li_4\&B_{36}$ show almost the same topological parameter as shown in Table 2. This indicates that the hydrogen is attached by the cluster in molecule form. The geometry of $Li_4\&B_{36}$ cluster is maintained after H_2 being attached comparing with isolated one. The molecular graph of $Li_4\&B_{36}$-H_2 is also shown in Fig. 2, from which one can find that one bond critical point between Li atom and H_2 molecule is localized. The corresponding electron density, and other topological parameters ($\nabla^2\rho$, H(r)) of Li-H_2 BCP suggest that the Li-H_2 interaction shows weak noncovalent characteristic. In addition, we note that the topological parameter of bond critical points relative to Li-B and B-B bonds in H_2-adsorbed species are almost the same to those of isolated $Li_4\&B_{36}$ cluster. This further demonstrates that the structure of host cluster was not distorted after H_2 being attached.

The nH_2-adsorbed configurations were extensively optimized to probe into the hydrogen storage stability. Vibrational frequency calculations confirmed that all the relaxed nH_2-adsorbed structures are to be local stable, and the Cartesian coordinates of these species are listed in Table S1 of supporting information. The relaxed configurations are depicted in Fig. 3. Our calculations indicate that each Li atom in $Li_4\&B_{36}$ cluster can attach six H_2 molecules at most. The average Li-B and B-B bond lengths of nH_2-adsorbed species are collected in Table 3, from which one can see that the B-B bond lengths in adsorbed species are not changed relative to the isolated cluster. On the other hand, the Li-B bonds are gradually elongated as the numbers of adsorbed H_2 molecules increase due to the increased interaction between Li atoms and H_2 molecules. The largest elongation of 0.025 Å is found for $(Li\text{-}6H_2)_4\&B_{36}$ species. Therefore, the H_2 adsorptions do not result into the high structure distortion of $Li_4\&B_{36}$ cluster. The bond lengths of adsorbed H_2 molecules are elongated by only 0.7% relative to the isolate H_2 molecule (0.774 Å). It is obvious that the H-H bonds are not broken after being adsorbed on $Li_4\&B_{36}$ cluster. The Li–H_2 distances are in a rather wide range from 2.207 Å to 3.080 Å as shown in Table 3. It is observable that there is an abrupt increase in the Li–H_2 bond lengths from $Li_4\&B_{36}$-$4H_2$ to $Li_4\&B_{36}$-$5H_2$, so that the first four H_2 molecules are closer to the Li site than the next one. By comparing $Li_4\&B_{36}$-$4H_2$ and $(Li\text{-}H_2)_4\&B_{36}$, one can find that the Li-B bonds are more elongated in $Li_4\&B_{36}$-$4H_2$ (4 H_2 coadsorption on one Li atom) than those in $(Li\text{-}H_2)_4\&B_{36}$ which corresponds to uniform adsorption on 4 Li atoms. Moreover, the adsorption energy of $(Li\text{-}H_2)_4\&B_{36}$ is significantly larger than that of $Li_4\&B_{36}$-$4H_2$. This indicates that the hydrogen molecules tend to uniformly be attached by 4 Li atoms.

We calculated consecutive adsorption energy (E_r) as the energy gained by successive additions of H_2 molecules to evaluate the reversibility for storage of H_2 molecules. The average adsorption energy (E_{ads}) was calculated to evaluate the adsorption capability of the $Li_4\&B_{36}$ cluster. They are defined as follows:

$$E_r = [E(Li_4\&B_{36} - (n-1)H_2) + E(H_2) - E(Li_4\&B_{36} - nH_2) \quad (1)$$

$$E_{ads} = [E(Li_4\&B_{36}) + nE(H_2) - E(Li_4\&B_{36} - nH_2)]/n \quad (2)$$

where, $E(Li_4\&B_{36})$, $E(H_2)$, $E(Li_4\&B_{36} - nH_2)$,$E(Li_4\&B_{36} - (n-1)H_2)$ are the total energy of $Li_4\&B_{36}$ cluster, H_2, $Li_4\&B_{36}$-nH_2, and $Li_4\&B_{36}$-(n-1)H_2, respectively. The E_r is an important index for testing the continuous hydrogen adsorption capacity of nanomaterials. The adsorption of H_2 is difficult if the E_r is negative[25], and the positive E_r means the spontaneous adsorption can occur between the hydrogen molecule and the $Li_4\&B_{36}$ structure. From Table 3, one can be found that the E_r for the sixth H_2 adsorbed by one Li atom is 0.04 eV. Therefore, we can conclude that each Li atom can at most attach six H_2 molecules in stable state. We note that a Li atom in Li-decorated B_{40} also attach six H_2 molecules at most in previous work[29]. The adsorption of 24 H_2 on the present system

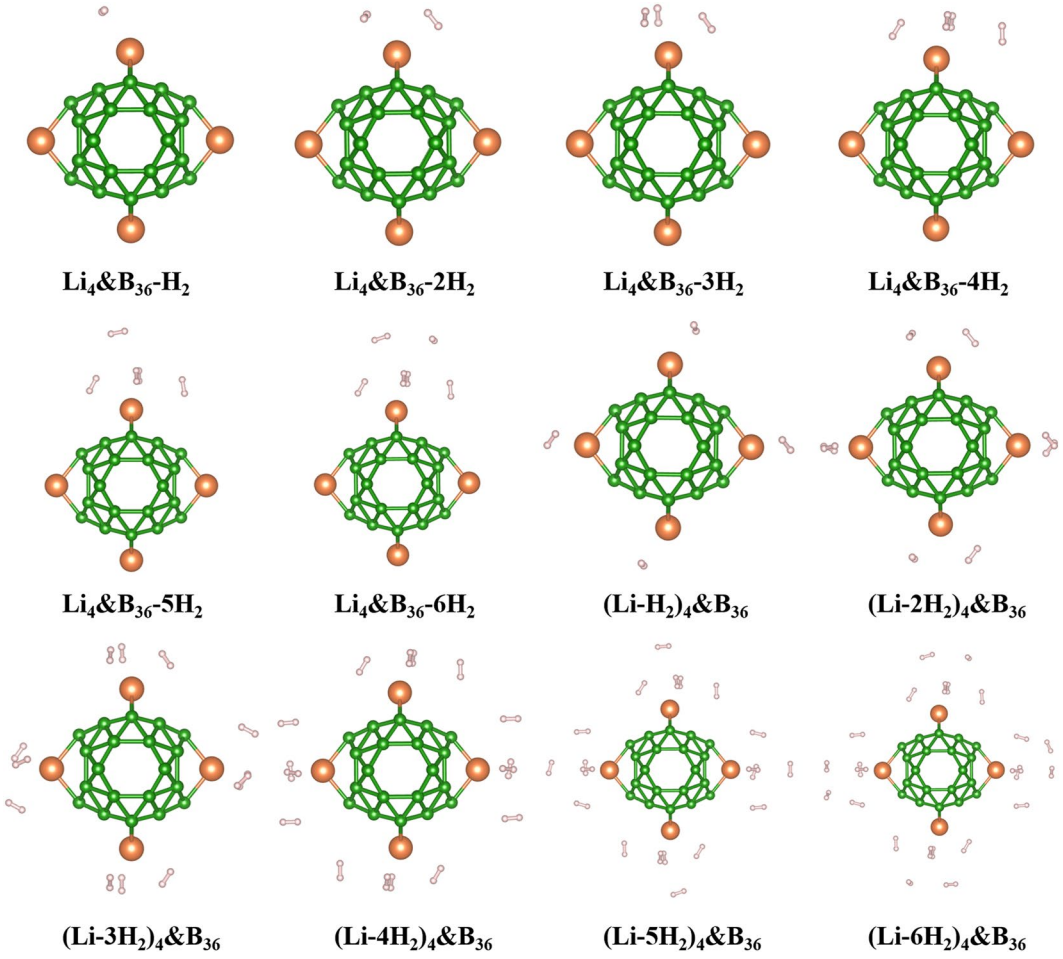

Figure 3. Optimized structure of H_2 molecules adsorbed $Li_4\&B_{36}$ cluster.

Species	$R_{Li\text{-}B}$(Å)	$R_{B\text{-}B}$(Å)	$R_{H\text{-}H}$(Å)	$R_{Li\text{-}H}$(Å)	Q_{Li}(e)	C_{Li}	E_{ads} (eV)	E_r (eV)
$Li_4\&B_{36}$-H_2	2.306	1.687	0.748	2.207	0.74	$1s^2 2s^0 2p^{0.20}$	0.14	0.14
$Li_4\&B_{36}$-$2H_2$	2.309	1.687	0.749	2.257	0.60	$1s^2 2s^0 2p^{0.30}$	0.13	0.12
$Li_4\&B_{36}$-$3H_2$	2.311	1.687	0.749	2.407	0.54	$1s^2 2s^0 2p^{0.36}$	0.11	0.07
$Li_4\&B_{36}$-$4H_2$	2.314	1.687	0.748	2.645	0.52	$1s^2 2s^0 2p^{0.37}$	0.10	0.07
$Li_4\&B_{36}$-$5H_2$	2.314	1.687	0.748	2.914	0.52	$1s^2 2s^0 2p^{0.37}$	0.09	0.04
$Li_4\&B_{36}$-$6H_2$	2.315	1.687	0.748	3.080	0.53	$1s^2 2s^0 2p^{0.37}$	0.08	0.04
$(Li\text{-}H_2)_4\&B_{36}$	2.305	1.687	0.749	2.218	0.73	$1s^2 2s^0 2p^{0.20}$	0.13	—
$(Li\text{-}2H_2)_4\&B_{36}$	2.309	1.687	0.749	2.258	0.60	$1s^2 2s^0 2p^{0.30}$	0.13	—
$(Li\text{-}3H_2)_4\&B_{36}$	2.326	1.687	0.749	2.416	0.54	$1s^2 2s^0 2p^{0.36}$	0.11	—
$(Li\text{-}4H_2)_4\&B_{36}$	2.327	1.687	0.748	2.674	0.53	$1s^2 2s^0 2p^{0.37}$	0.10	—
$(Li\text{-}5H_2)_4\&B_{36}$	2.330	1.687	0.748	2.935	0.53	$1s^2 2s^0 2p^{0.37}$	0.08	—
$(Li\text{-}6H_2)_4\&B_{36}$	2.331	1.687	0.748	3.011	0.53	$1s^2 2s^0 2p^{0.36}$	0.08	

Table 3. Calculated structural parameters, NPA charge (Q_{Li}) and electron configuration (C_{Li}) of Li atom, adsorption energy (E_{ads}) and consecutive adsorption energy (E_r) of H_2-adsorbed $Li_4\&B_{36}$ species.

($Li_4\&B_{36}$) corresponds to a gravimetric density of 10.4%. It is obvious that the gravimetric density exceeds the 5.5 wt% at 2017 specified by the US department of energy (DOE). It can be seen from Table 3 that the E_{ads} are in the range of 0.08eV–0.14 eV calculated at the *w*B97*x*/6-311++g(2d, 2p) level of theory. These values are very close to the average bonding energy for lithium coated fullerene $Li_{12}C_{60}$[14], aromatic B_6Li_8[19] complex, and lithium-decorated borospherene Li_6B_{40}[29].

It can be seen from Table 3 that the Li atoms in all nH_2-adsorbed species act as electron donor, and the charge transfer is decreased as the numbers of adsorbed H_2 molecules increase. In addition, the 2s→2p electron

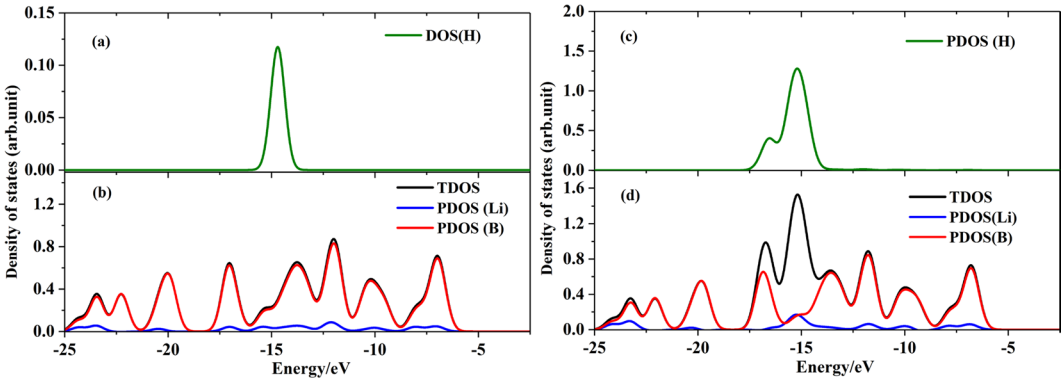

Figure 4. Partial density of states (PDOS) of isolated H_2 (**a**) and $Li_4\&B_{36}$ (**b**), adsorbed H_2 (**c**) and $Li_4\&B_{36}$ (**d**) in $Li_4\&B_{36}$-$20H_2$ complex.

promotion occurs in the Li atoms after H_2 being adsorbed, which results into the non-empty occupancy in 2p orbital (0.20–0.37e) of Li atoms.

Partial density of states (PDOS) of free H_2 and $Li_4\&B_{36}$ and $20H_2$-adsorbed $(Li\text{-}5H_2)_4\&B_{36}$ complexes are analyzed to understand the bonding characteristics of hydrogen adsorbed systems. The PDOS plots are depicted in Fig. 4. For $Li_4\&B_{36}$ cluster, there exists very weak orbital overlaps between B and Li atoms, which is in agreement with the ionic characters revealed by aforementioned QTAIM analyses. Comparing to the free $Li_4\&B_{36}$ cluster, there exists new peak around −15eV in the $20H_2$-adsorbed complex, stemming from the 2p electron of Li atoms due to the 2 s→2p electron promotion. Additionally, the new peak can participate into the orbital overlaps with H_2 molecules. This results into the physical interaction between H_2 molecules and $Li_4\&B_{36}$ cluster.

Conclusion

The Saturn-like charge-transfer complexes $Li_4\&B_{36}$ cluster were investigated as a candidate for hydrogen storage with density functional theory (DFT) methods. The bonding nature in bare and H_2-adsorbed $Li_4\&B_{36}$ clusters was revealed with QTAIM analyses. Our results suggest that each face-capping Li atom donates about one electron to the electron-deficient B_{36} core, resulting into the $(Li^+)_4B_{36}{}^{4-}$ charge-transfer complex. The ionic characters of Li-B bonds and covalent characters of B-B bonds are understood for bare $Li_4\&B_{36}$ cluster. Each Li atom in $Li_4\&B_{36}$ cluster can at most attach five H_2 molecules, which results into the gravimetric density of 10.4%, exceeding the 5.5 wt% at 2017 specified by the US department of energy (DOE). The structure distortion of $Li_4\&B_{36}$ cluster was not occurred after the H_2 molecules were attached. The adsorption energies of H_2 molecules on $Li_4\&B_{36}$ cluster are in the range of 0.08-0.14 eV at the *w*B97*x*/6-311++g(2d, 2p) level of theory. These values are very close to the average bonding energy for lithium coated fullerene $Li_{12}C_{60}$, aromatic B_6Li_8 complex and lithium-decorated borospherene Li_6B_{40}. Our study indicates that the $Li_4\&B_{36}$ cluster may be appropriate material for hydrogen storage, but also need further confirmation in experiment.

Method

All the calculations were carried out with G09 package[43]. The molecular structures of bare and nH_2-adsorbed $Li_4\&B_{36}$ species were fully relaxed without any symmetry constrains using *w*B97*x* functional[33]. This functional has considered the long-rang corrections, and is proved to be reliable methods to predict non-covalent interactions. The classical extended basis set 6-31 g (d, p) was utilized in the geometry optimization. By adding H_2 molecules around the Li atoms to construct the starting adsorption configurations of $Li_4\&B_{36}$-nH_2 (n=1–20) which were then full relaxed at the *w*B97*x*/6-31 G(d, p) level of theory. The harmonic vibrational frequency calculations were carried out at the same level of theory to guarantee that the optimized structures correspond to local minima on the potential energy surface. The larger basis set, 6-311++g(2d, 2p), was employed in the single-point energy calculations to obtain the more reasonable adsorption energy.

To understand the bonding characters of the studied systems, the quantum theory of atoms in molecules (QTAIM)[37] and natural population analyses (NPA)[34] were performed with MULTIWFN program[44].

References

1. Schlapbach, L. & Züttel, A. Hydrogen-storage materials for mobile applications. *Nature.* **414**, 353–358 (2001).
2. Jena, P. Materials for Hydrogen Storage: Past, Present, and Future. *J. Phys. Chem. Lett.* **2**, 206 (2011).
3. Grochala, W. & Edwards, P. P. Thermal Decomposition of the Non-Interstitial Hydrides for the Storage and Production of Hydrogen. *Chem. Rev.* **104**, 1283–1315 (2004).
4. Orimo, S., Nakamori, Y., Eliseo, J. R., Züttel, A. & Jensen, C. M. Complex Hydrides for Hydrogen Storage. *Chem. Rev.* **107**, 4111–4132 (2007).
5. Dillon, A. C. *et al.* Storage of hydrogen in single-walled carbon nanotubes. *Nature.* **386**, 377–379 (1997).
6. Yürüm, Y., Taralp, A. & Veziroglu, T. N. Storage of hydrogen in nanostructured carbon materials. *Int. J. Hydrogen Energy.* **34**, 3784–3798 (2009).
7. Yildirim, T., Íñguez, J. & Ciraci, S. Molecular and dissociative adsorption of multiple hydrogen molecules on transition metal decorated C_{60}. *Phys. Rev.* B. **72**, 153403 (2005)
8. Sun, Q., Wang, Q., Jena, P. & Kawazoe, Y. Clustering of Ti on a C_{60} surface and its effect on hydrogen storage. *J. Am. Chem. Soc* **127**, 14582–14583 (2005).

9. Yildirim, T. & Ciraci, S. Titanium-decorated carbon nanotubes as a potential high-capacity hydrogen storage medium. *Phys. Rev. Lett* **94**, 175501 (2005).
10. Shalabi, A. S., Abdel Aal, S., Assem, M. M. & Abdel Halim, W. S. Ab initio characterization of Ti decorated SWCNT for hydrogen storage. *Int. J. Hydrogen Energy* **38**, 140–152 (2013).
11. Ma, L. J., Jia, J. F., Wu, H. S. & Ren, Y. Ti-η^2-(C_2H_2) and HC≡C-TiH as high capacity hydrogen storage media. *Int. J. Hydrogen Energy* **38**, 16185–16192 (2013).
12. Bora, P. L., Ahmad, R. & Singh, A. K. Remarkable enhancement in hydrogen storage on free-standing Ti_3B and BC_3 supported Ti_3 clusters. *Int. J. Hydrogen Energy* **40**, 1054–1061 (2015).
13. Tang, C. M. *et al*. Transition metal Ti coated porous fullerene $C_{24}B_{24}$: potential material for hydrogen storage. *Int. J. Hydrogen Energy* **40**, 16271–16277 (2015).
14. Sun, Q., Jena, P., Wang, Q. & Marquez, M. First-Principles Study of Hydrogen Storage on $Li_{12}C_{60}$. *J. Am. Chem. Soc.* **128**, 9741–9745 (2006).
15. Yoon, M. *et al*. Calcium as the superior coating metal in functionalization of carbon fullerenes for high-capacity hydrogen storage. *Phys. Rev. Lett*. **100**, 206806 (2008)
16. Teprovich, J. A. Jr. *et al*. Synthesis and characterization of a lithium-doped fullerene (Li_x-C_{60}-H_y) for reversible hydrogen storage. *Nano Lett*. **12**, 582–589 (2012).
17. Mauron, P. *et al*. Hydrogen Sorption in $Li_{12}C_{60}$. *J. Phys. Chem. C.* **117**, 22598–22602 (2013).
18. Pan, S., Merino, G. & Chattaraj, P. K. The hydrogen trapping potential of some Li-doped star-like clusters and super-alkali systems. *Phys. Chem. Chem. Phys* **14**, 10345–10350 (2012).
19. Ba Tai, T. & Nguyen, M. T. Three-dimensional aromatic B_6Li_8 complex as a high capacity hydrogen storage material. *Chem Commun* **49**, 913–915 (2013).
20. Tang, C. M., Wang, Z. G., Zhang, X. & Wen, N. H. The hydrogen storage properties of Na decorated small boron cluster B_6Na_8. *Chem. Phys. Lett.* **661**, 161–167 (2016).
21. Du, J. G., Sun, X. Y., Jiang, G. & Zhang, C. Y. The hydrogen storage on heptacoordinate carbon motif CTi_7^{2+}. *Int. J. Hydrogen Energy* **41**, 11301–11307 (2016).
22. Li, Y. C., Zhou, G., Li, J., Gu, B. L. & Duan, W. H. Alkali-metal-doped B_{80} as high-capacity hydrogen storage media. *J. Phys. Chem. C.* **112**, 19268–19271 (2008).
23. Li, M., Li, Y. F., Zhou, Z., Shen, P. W. & Chen, Z. F. Ca-coated boron fullerenes and nanotubes as superior hydrogen storage materials. *Nano. Lett.* **9**, 1944–1948 (2009).
24. Li, J. L., Hu, Z. S. & Yang, G. W. High-capacity hydrogen storage of magnesium-decorated boron fullerene. *Chem. Phys* **392**, 16–20 (2012).
25. Wu, G. F., Wang, J. L., Zhang, X. Y. & Zhu, L. Y. Hydrogen storage on metal-coated B_{80} buckyballs with density functional theory. *J. Phys. Chem. C.* **113**, 7052–7057 (2009).
26. De, S. *et al*. Energy Landscape of Fullerene Materials: A Comparison of Boron to Boron Nitride and Carbon. *Phys. Rev. Lett.* **106**, 225502 (2011).
27. Li, F. Y. *et al*. B_{80} and $B_{101\text{-}103}$ clusters: Remarkable stability of the core-shell structures established by validated density functionals. *J. Chem. Phys.* **136**, 074302 (2012).
28. Zhai, H. J. *et al*. Observation of an all-boron fullerene. *Nat. Chem.* **6**, 727–731 (2014).
29. Bai, H. *et al*. Bai B, Lithium-Decorated Borospherene B_{40}: A Promising Hydrogen Storage Medium. *Sci. Rep.* **6**, 35518 (2016).
30. Dong, H. L., Hou, T. J., Lee, S. T. & Li, Y. Y. New Ti-decorated B_{40} fullerene as a promising hydrogen storage material. *Sci. Rep.* **5**, 09952 (2015).
31. Piazza, Z. A. *et al*. Planar hexagonal B_{36} as a potential basis for extended single-atom layer boron sheets. *Nat. Commun.* **5**, 3113 (2014).
32. Tian, W. J. *et al*. Saturn-like charge-transfer complexes Li_4&B_{36}, Li_5&B_{36}^+, and Li_6&B_{36}^{2+}: exohedral metalloborospherenes with a perfect cage-like B_{36}^{4-} core. *Phys. Chem. Chem. Phys.* **18**, 9922–9926 (2016).
33. Chai, J. D. & Head-Gordon, M. Long-range corrected hybrid density functionals with damped atom-atom dispersion corrections. *Phys. Chem. Chem. Phys.* **10**, 6615–6620 (2008).
34. Foster, J. P. & Weinhold, F. Natural hybrid orbitals. *J. Am. Chem. Soc.* **102**, 7211–7218 (1980).
35. Schleyer, P. V., Maerker, C., Dransfeld, A., Jiao, H. J. & Hommes, N. J. R. V. Nucleus-Independent Chemical Shifts: A Simple and Efficient Aromaticity Probe. *J. Am. Chem. Soc.* **118**, 6317–6318 (1996).
36. Hoffmann, R., Schleyer, P. V. & Schaefer, H. F. Predicting Molecules-More Realism, Please! *Angew. Chem., Int. Ed.* **47**, 7164–7167 (2008).
37. Bader, R. W. F. Atoms in molecules: a quantum theory. Oxford: Clarendon; 1990.
38. Cremer, D. & Kraka, E. Chemical bonds without bonding electron density-does the difference electron-density analysis suffice for a description of the chemical bond? *Angew Chem, Int Ed.* **23**, 627–628 (1984).
39. Mayer, I. & Salvador, P. Overlap populations, bond orders and valences for 'fuzzy' atoms. *Chem. Phys. Lett.* **383**, 368–375 (2004).
40. Becke, A. D. & Edgecombe, K. E. A simple measure of electron localization in atomic and molecular systems. *J. Chem. Phys.* **92**, 5397–5403 (1990).
41. Silvi, B. & Savin, A. Classification of chemical bonds based on topological analysis of electron localization functions. *Nature.* **371**, 683–686 (1994).
42. Dekock, R. L. & Gray, H. B. Chemical structure and bonding. University Science Books; (1989).
43. Frisch, M. J. *et al*. Gaussian 09, revision B.01. Wallingford, CT: Gaussian, Inc., (2009).
44. Lu, T. & Chen, F. W. Multiwfn: a multifunctional wavefunction analyzer. *J. Comp. Chem.* **33**, 580–592 (2012).

Acknowledgements

This work is supported by National Natural Science Foundation of China (Grant NO.11204193, Grant No.11404042).

Author Contributions

Jiguang Du conceived the main idea, analyzed the results and wrote the manuscript. Xiyuan Sun and Li Zhang performed all the calculation works. Chuanyu Zhang and Gang Jiang participated in the discussions and all authors contributed to revisions.

Additional Information

Supplementary information accompanies this paper at https://doi.org/10.1038/s41598-018-20452-8.

Competing Interests: The authors declare that they have no competing interests.

Publisher's note: Springer Nature remains neutral with regard to jurisdictional claims in published maps and institutional affiliations.